Supplemental Information for

Phosphorylation Toggles the SARS-CoV-2 Nucleocapsid Protein Between Two Membrane-Associated Condensate States

Bruna Favetta[1], Huan Wang[2], Jasmine Cubuk[3], Mayur Barai[4], Cesar Ramirez[1], Adam J. Gormley[1], Sanjeeva Murthy[2], Andrea Soranno[3], Zheng Shi[2], Benjamin S. Schuster[4]

1 Department of Biomedical Engineering, Rutgers, The State University of New Jersey, Piscataway, NJ 08854
2 Department of Chemistry and Chemical Biology, Rutgers, The State University of New Jersey, Piscataway, NJ 08854
3 Department of Biochemistry and Molecular Biophysics, Washington University in St. Louis, St. Louis, MO 63110
4 Department of Chemical and Biochemical Engineering, Rutgers, The State University of New Jersey, Piscataway, NJ 08854

Corresponding author:
Benjamin S. Schuster. Email: benjamin.schuster@rutgers.edu

This PDF file includes:

Supporting Table 1

Coding sequence for proteins, oligonucleotides, and recombinant DNA used in this study

Name	Sequence
SARS-COV-2 Nucleocapsid (N) protein	ATGCATCACCACCATCATCATGAGAATTTATATTTCCAGGGCAGCGATAACG GCCCGCAGAATCAGCGCAACGCGCCGCGCATTACCTTTGGCGGCCCGAG CGATAGCACCGGCAGCAACCAAAACGGAGAGCGCAGCGGCGCGCGCAG CAAACAACGCCGCCCCCAAGGCCTGCCGAACAACACCGCGAGCTGGTTT ACCGCGCTGACGCAGCATGGCAAAGAAGATCTGAAATTTCCGCGCGGCC AAGGCGTGCCGATTAACACCAACAGCAGCCCGGATGATCAGATTGGCTAT TATCGCCGCGCGACCCGCCGCATTCGCGGCGGCGATGGCAAAATGAAAG ATCTGAGCCCGCGCTGGTATTTTTATTATCTGGGCACCGGCCCGGAAGCG GGCCTGCCGTATGGCGCGAACAAAGATGGCATTATTTGGGTGGCGACCG AAGGCGCGCTGAACACCCCGAAAGATCATATTGGCACCCGCAACCCGGC GAACAACGCGGCGATTGTGCTGCAGCTGCCGCAAGGCACCACCCTGCC GAAAGGCTTCTATGCCGAAGGTTCGCGCGGAGGGAGCCAAGCGTCATCA CGCAGCAGCAGCCGTTCGAGGAACAGCAGCCGCAACAGCACTCCCGGG AGTTCCCGTGGCACATCGCCGGCGCGTATGGCGGGCAATGGCGGGGAC GCAGCGCTGGCGCTGCTGCTGCTGGATCGCCTGAATCAGCTGGAAAGCA AAATGAGCGGCAAAGGTCAGCAGCAGCAAGGCCAAACCGTAACGAAAAA AAGCGCGGCGGAAGCGAGCAAAAAACCGCGTCAGAAACGCACCGCGAC CAAAGCGTATAACGTGACCCAAGCGTTTGGCCGCCGCGGCCCGGAACAG ACCCAAGGCAACTTTGGCGATCAAGAACTGATTCGCCAAGGCACCGATTA TAAACATTGGCCGCAGATTGCGCAGTTTGCGCCGAGCGCGAGCGCGTTT TTTGGCATGAGCCGCATTGGCATGGAAGTGACCCCGAGCGGCACCTGGC TGACCTATACCGGCGCGATTAAACTGGATGATAAAGATCCGAACTTTAAAG ATCAAGTGATTCTGCTGAACAAACATATTGATGCGTATAAAACCTTTCCGCC GACCGAACCGAAAAAAGATAAAAAAAAAAAAAGCGGATGAAACCCAAGCGC TGCCGCAGCGTCAGAAAAAACAGCAGACCGTTACACTGCTGCCGGCGGC GGATCTGGATGATTTTAGCAAACAGCTGCAGCAGAGCATGAGCAGCGCG GATAGCACCCAAGCG
SL4 RNA FAM labeled	FAM – 5’ CUGUGUGGCUGUCACUCGGCUGCAUGCUUAGUGCACUCACGCAG – 3’
polyA RNA FAM labeled	FAM – 5’ AAAAAAAAAAAAAAAAAAAAAAAAAAAAA – 3’
1-1000 RNA	GGGTTAAAGGTTTATACCTTCCCAGGTAACAAACCAACCAACTTTCGATCT CTTGTAGATCTGTTCTCTAAACGAACTTTAAAATCTGTGTGGCTGTCACTC GGCTGCATGCTTAGTGCACTCACGCAGTATAATTAATAACTAATTACTGTCG TTGACAGGACACGAGTAACTCGTCTATCTTCTGCAGGCTGCTTACGGTTTC GTCCGTGTTGCAGCCGATCATCAGCACATCTAGGTTTCGTCCGGGTGTGA CCGAAAGGTAAGATGGAGAGCCTTGTCCCTGGTTTCAACGAGAAAACACA CGTCCAACTCAGTTTGCCTGTTTTACAGGTTCGCGACGTGCTCGTACGTG GCTTTGGAGACTCCGTGGAGGAGGTCTTATCAGAGGCACGTCAACATCTT AAAGATGGCACTTGTGGCTTAGTAGAAGTTGAAAAAGGCGTTTTGCCTCA ACTTGAACAGCCCTATGTGTTCATCAAACGTTCGGATGCTCGAACTGCAC CTCATGGTCATGTTATGGTTGAGCTGGTAGCAGAACTCGAAGGCATTCAGT ACGGTCGTAGTGGTGAGACACTTGGTGTCCTTGTCCCTCATGTGGGCGA AATACCAGTGGCTTACCGCAAGGTTCTTCTTCGTAAGAACGGTAATAAAGG AGCTGGTGGCCATAGTTACGGCGCCGATCTAAAGTCATTTGACTTAGGCG ACGAGCTTGGCACTGATCCTTATGAAGATTTTCAAGAAAACTGGAACACTA AACATAGCAGTGGTGTTACCCGTGAACTCATGCGTGAGCTTAACGGAGGG GCATACACTCGCTATGTCGATAACAACTTCTGTGGCCCTGATGGCTACCCT CTTGAGTGCATTAAAGACCTTCTAGCACGTGCTGGTAAAGCTTCATGCACT TTGTCCGAACAACTGGACTTTATTGACACTAAGAGGGGTGTATACTGCTGC

	CGTGAACATGAGCATGAAATTGCTTGGTACACGGAACGTTCTGGGCCCTC GA
N RNA	GGGTTAAAGGTTTATACCTTCCCAGGTAACAAACCAACCAACTTTCGATCT CTTGTAGATCTGTTCTCTAAACGAACAAACTAAAATGTCTGATAATGGACCC CAAAATCAGCGAAATGCACCCCGCATTACGTTTGGTGGACCCTCAGATTC AACTGGCAGTAACCAGAATGGAGAACGCAGTGGGGCGCGATCAAAACAA CGTCGGCCCCAAGGTTTACCCAATAATACTGCGTCTTGGTTCACCGCTCT CACTCAACATGGCAAGGAAGACCTTAAATTCCCTCGAGGACAAGGCGTTC CAATTAACACCAATAGCAGTCCAGATGACCAAATTGGCTACTACCGAAGAG CTACCAGACGAATTCGTGGTGGTGACGGTAAAATGAAAGATCTCAGTCCA AGATGGTATTTCTACTACCTAGGAACTGGGCCAGAAGCTGGACTTCCCTAT GGTGCTAACAAAGACGGCATCATATGGGTTGCAACTGAGGGAGCCTTGAA TACACCAAAAGATCACATTGGCACCCGCAATCCTGCTAACAATGCTGCAAT CGTGCTACAACTTCCTCAAGGAACAACATTGCCAAAAGGCTTCTACGCAG AAGGGAGCAGAGGCGGCAGTCAAGCCTCTTCTCGTTCCTCATCACGTAG TCGCAACAGTTCAAGAAATTCAACTCCAGGCAGCAGTAGGGGAACTTCTC CTGCTAGAATGGCTGGCAATGGCGGTGATGCTGCTCTTGCTTTGCTGCTG CTTGACAGATTGAACCAGCTTGAGAGCAAAATGTCTGGTAAAGGCCAACA ACAACAAGGCCAAACTGTCACTAAGAAATCTGCTGCTGAGGCTTCTAAGA AGCCTCGGCAAAAACGTACTGCCACTAAAGCATACAATGTAACACAAGCTT TCGGCAGACGTGGTCCAGAACAAACCCAAGGAAATTTTGGGGACCAGGA ACTAATCAGACAAGGAACTGATTACAAACATTGGCCGCAAATTGCACAATT TGCCCCCAGCGCTTCAGCGTTCTTCGGAATGTCGCGCATTGGCATGGAA GTCACACCTTCGGGAACGTGGTTGACCTACACAGGTGCCATCAAATTGGA TGACAAAGATCCAAATTTCAAAGATCAAGTCATTTTGCTGAATAAGCATATT GACGCATACAAAACATTCCCACCAACAGAGCCTAAAAAGGACAAAAAGAA GAAGGCTGATGAAACTCAAGCCTTACCGCAGAGACAGAAGAAACAGCAAA CTGTGACTCTTCTTCCTGCTGCAGATTTGGATGATTTCTCCAAACAATTGC AACAATCCATGAGCAGTGCTGACTCAACTCAGG
Primer 1-1000 Forward	CCATCCGGCGTAATACGACTCACTATAGGG
Primer 1-1000 Reverse	CTAGAAAGATAGAACGTTCCGTGTACCAAG
Primer N Forward	GTGTGATGGATATCTGCAGAATTCGC
Primer N Reverse	CATGAGTTTAGGCCTGAGTTGAGTCAG
6xHis-GFP-M(104-222)	ATGGGTTCTTCTCACCATCACCATCACCATGGTTCTTCTGTGAGCAAGGG CGAGGAGCTGTTCACCGGGGTGGTGCCCATCCTGGTCGAGCTGGACGG CGACGTAAACGGCCACAAGTTCAGCGTGCGCGGCGAGGGCGAGGGCGA TGCCACCAACGGCAAGCTGACCCTGAAGTTCATCTGCACCACCGGCAAG CTGCCCGTGCCCTGGCCCACCCTCGTGACCACCCTGACCTACGGCGTGC AGTGCTTCAGCCGCTACCCCGACCACATGAAGCAGCACGACTTCTTCAAG TCCGCCATGCCCGAAGGCTACGTCCAGGAGCGCACCATCTCCTTCAAGG ACGACGGCACCTACAAGACCCGCGCCGAGGTGAAGTTCGAGGGCGACA CCCTGGTGAACCGCATCGAGCTGAAGGGCATCGACTTCAAGGAGGACGG CAACATCCTGGGGCACAAGCTGGAGTACAACTTCAACAGCCACAACGTCT ATATCACGGCCGACAAGCAGAAGAACGGCATCAAGGCGAACTTCAAGATC CGCCACAACGTCGAGGACGGCAGCGTGCAGCTCGCCGACCACTACCAG CAGAACACCCCCATCGGCGACGGCCCCGTGCTGCTGCCCGACAACCACT ACCTGAGCACCCAGTCCAAGCTGAGCAAAGACCCCAACGAGAAGCGCGA TCACATGGTCCTGCTGGAGTTCGTGACCGCCGCCGGGATCACTCTCGGC ATGGACGAGCTGTACAAGGGGATCGAGGAAAACCTGTACTTCCAATCCAA TGCAGCTCGCACACGCAGTATGTGGTCCTTTAACCCGGAGACCAATATTCT

	TCTGAACGTCCCCTTGCATGGTACTATCCTTACCCGCCCCCTTCTGGAGA GTGAACTGGTGATCGGTGCCGTCATCTTACGTGGGCATTTACGCATCGCG GGGCACCACTTAGGGCGCTGTGACATTAAAGACTTACCCAAGGAAATTAC TGTAGCTACTTCGCGTACTCTTTCCTATTATAAGTTAGGCGCATCACAGCGC GTGGCGGGCGATTCTGGCTTTGCAGCATATTCACGCTACCGCATTGGGAA TTATAAATTAAATACAGATCACTCAAGTTCCTCCGATAACATCGCCCTGTTG GTACAG
6xHis-GFP-Nsp3Ubl1	ATGGGTTCTTCTCACCATCACCATCACCATGGTTCTTCTGTGAGCAAGGG CGAGGAGCTGTTCACCGGGGTGGTGCCCATCCTGGTCGAGCTGGACGG CGACGTAAACGGCCACAAGTTCAGCGTGCGCGGCGAGGGCGAGGGCGA TGCCACCAACGGCAAGCTGACCCTGAAGTTCATCTGCACCACCGGCAAG CTGCCCGTGCCCTGGCCCACCCTCGTGACCACCCTGACCTACGGCGTGC AGTGCTTCAGCCGCTACCCCGACCACATGAAGCAGCACGACTTCTTCAAG TCCGCCATGCCCGAAGGCTACGTCCAGGAGCGCACCATCTCCTTCAAGG ACGACGGCACCTACAAGACCCGCGCCGAGGTGAAGTTCGAGGGCGACA CCCTGGTGAACCGCATCGAGCTGAAGGGCATCGACTTCAAGGAGGACGG CAACATCCTGGGGCACAAGCTGGAGTACAACTTCAACAGCCACAACGTCT ATATCACGGCCGACAAGCAGAAGAACGGCATCAAGGCGAACTTCAAGATC CGCCACAACGTCGAGGACGGCAGCGTGCAGCTCGCCGACCACTACCAG CAGAACACCCCCATCGGCGACGGCCCCGTGCTGCTGCCCGACAACCACT ACCTGAGCACCCAGTCCAAGCTGAGCAAAGACCCCAACGAGAAGCGCGA TCACATGGTCCTGCTGGAGTTCGTGACCGCCGCCGGGATCACTCTCGGC ATGGACGAGCTGTACAAGGGGATCGAGGAAAACCTGTACTTCCAATCCAA TGCATCTTCTAATGGCGCACCGACAAAAGTTACATTTGGAGACGATACCGT GATCGAAGTTCAGGGCTACAAAAGCGTGAACATCACCTTCGAGCTGGATG AACGTATCGATAAAGTGCTGAACGAGAAATGCAGCGCATATACCGTGGAAC TGGGTACCGAAGTGAACGAATTTGCCTGTGTTGTTGCAGATGCAGTGATC AAAACCTTACAGCCGGTTAGCGAACTGCTGACACCTTTAGGCATTGATCTG GATGAATGGAGCATGGCAACCTATTATCTGTTCGACGAAAGCGGCGAGTT CAAACTGGCATCACACATGTATTGCAGCTTCTATCCGCCTGATGAA

Supplemental Figures

A. Unmodified N, theoretical mass: 47300.46 Da

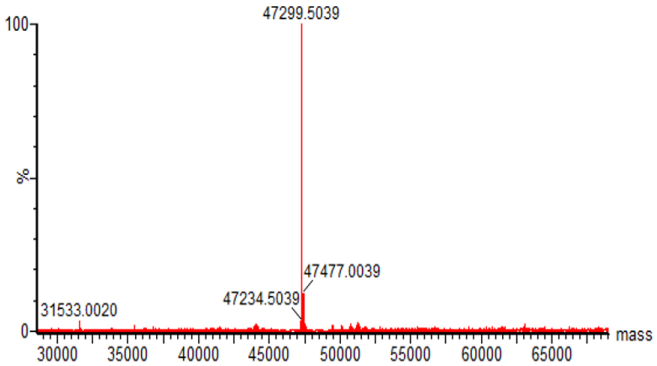

Phosphorylated N

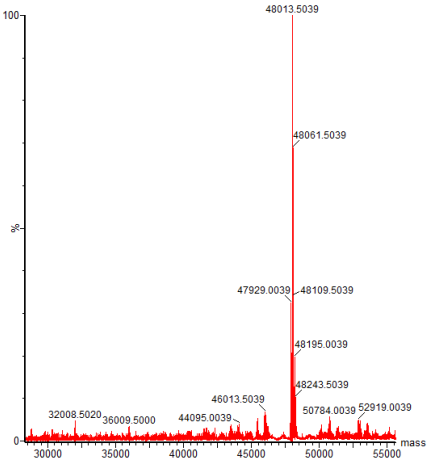

B.

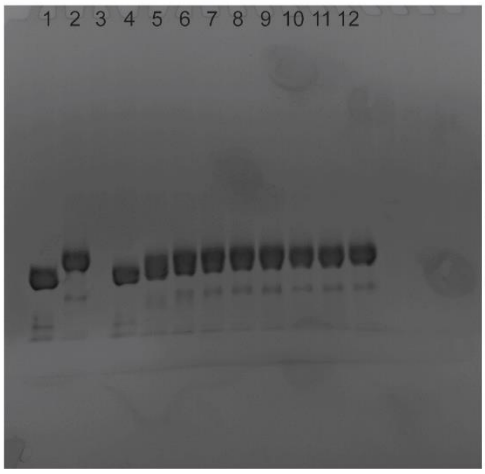

1. N
2. N + SRPK + GSK3β + Rxn buffer + 120 min
3. Empty
4. Rxn mixture at 0 min
5. Rxn mixture at 15 min
6. Rxn mixture at 30 min
7. Rxn mixture at 45 min
8. Rxn mixture at 60 min
9. Rxn mixture at 75 min
10. Rxn mixture at 90 min
11. Rxn mixture at 105 min
12. Rxn mixture at 120 min

Figure S1. Confirmation of N protein Phosphorylation. A) LC-MS profile for N protein prior to phosphorylation and following phosphorylation showing a mass increase of the main peak from 47.3 kDa to 48.0 kDa. This mass increase likely represents the addition of 9 (+ 720 Da) phosphate groups. B) SuperSep Phos-tag SDS-PAGE of N protein sample before, after, and during phosphorylation reaction at the timepoints indicated.

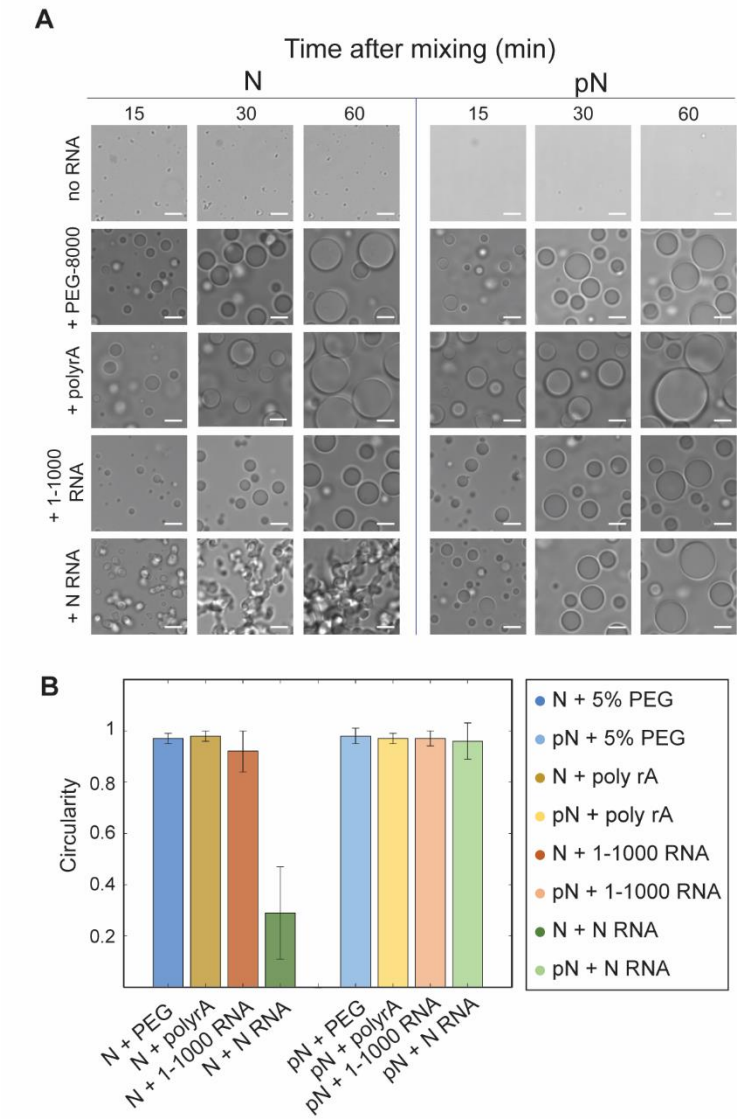

Figure S2. Characterization of morphology of N condensate samples. A) Representative images from the formation of condensates over time with N or pN protein – without RNA, with a crowding agent (5% PEG8000), with unstructured polyA RNA or with viral RNA fragments. Droplet morphology depends on protein and RNA combination. Scale bar = 5 µm. B) Quantification of droplet morphology from A. Circularity of droplets at 60 minutes was measured as $\boldsymbol{C = (4\pi * area/perimeter^2) * (1 - 0.5/r)^2}$ where $\boldsymbol{r = perimeter/2\pi}$. All protein and RNA combinations have a circularity ~ 1 except for condensates formed from N protein and N RNA. (n = 5 independent trials).

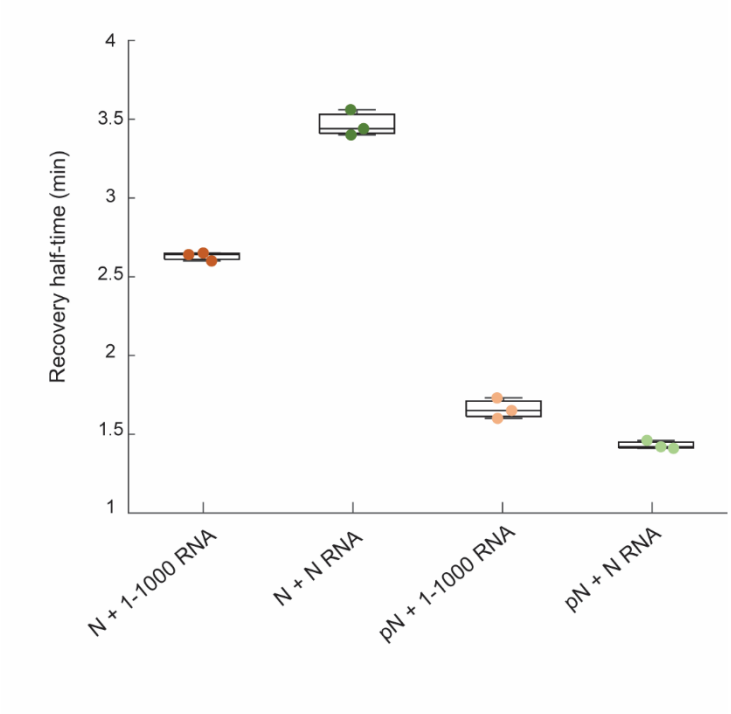

Figure S3. Recovery half times quantified from fluorescence recovery after photobleaching (FRAP) experiments. FRAP recovery curves following protein bleaching were fit to a simple exponential model. Phosphorylation reduces the recovery half time of N protein in condensates, indicating an increase in the diffusion of N. Data represents 3 independent trials.

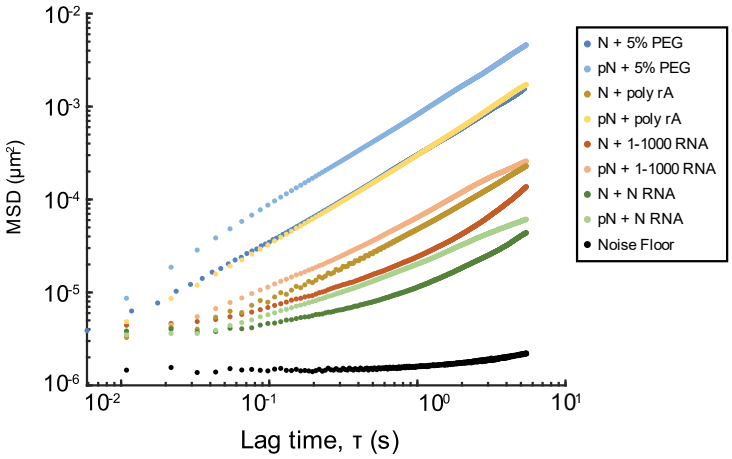

Figure S4. Noise floor for the MSD data shown in Figure 4D. Ensemble MSD versus lag time for the protein and RNA combinations tested in this study, including the noise floor in black. The noise floor was calculated as the average of 12 videos from 3 independent trials. The experimental setup includes a microfluidic temperature controller (Cherry Biotech) that causes vibrations resulting in noise.

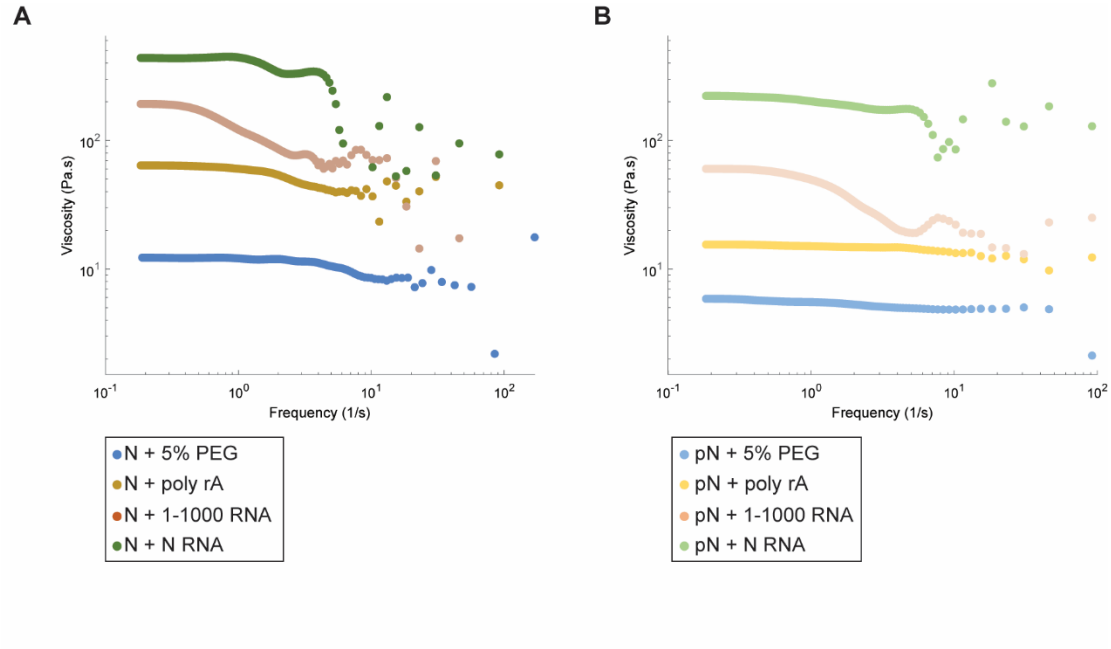

Figure S5. The viscosity of N condensates as a function of frequency as obtained from the microrheology experiments. These results were used to calculate the zero-shear viscosities plotted in Figure 4 and S9.

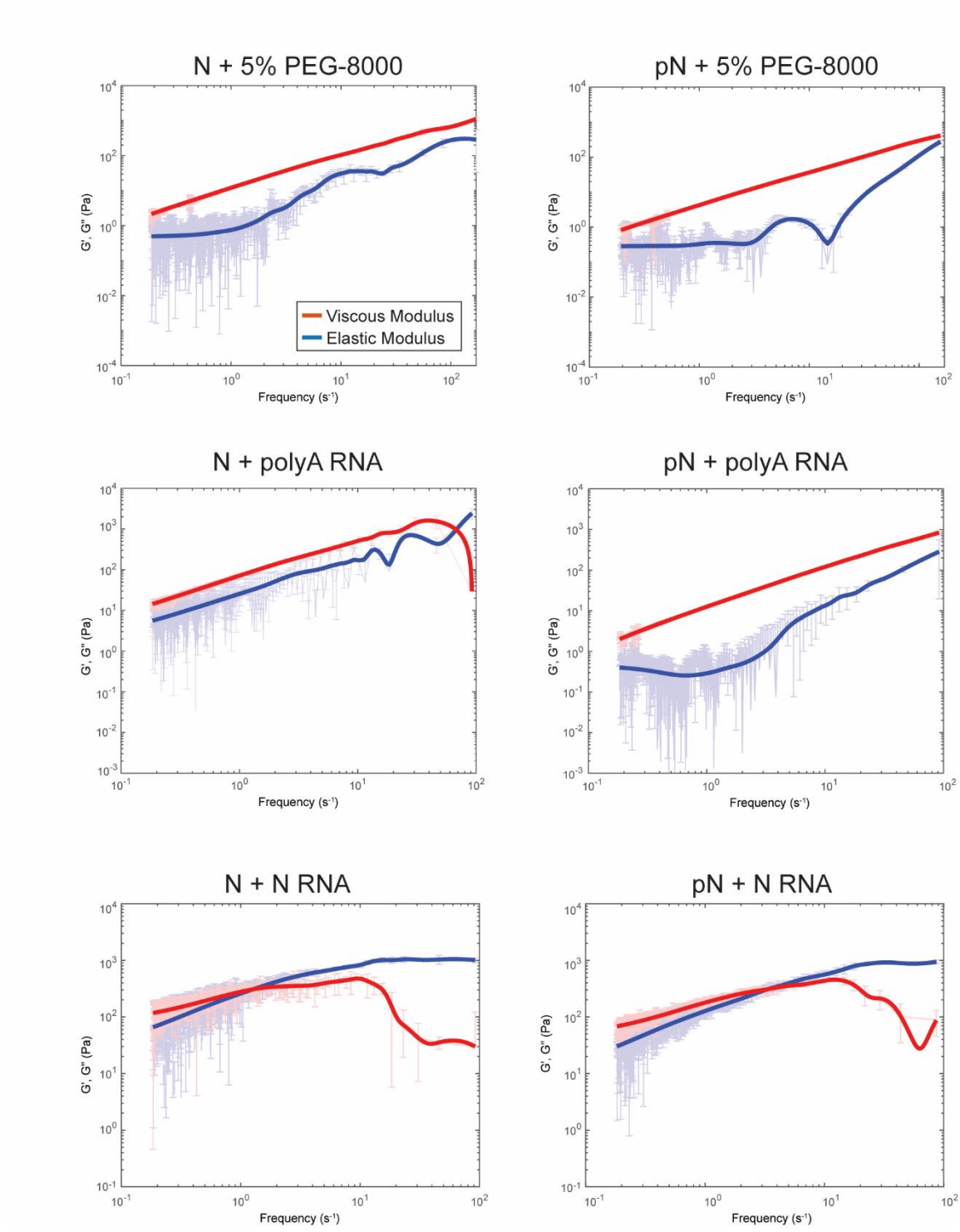

Figure S6. Frequency-dependent viscous and elastic moduli for N vs. pN condensates not shown in Figure 4. Plot with the average frequency-dependent viscous modulus (G'', red) and elastic modulus (G', blue) of N/pN + 5% PEG or N/pN + 1 mg/mL polyA RNA or N/pN + 300 nM N RNA condensates. Data is calculated from the MSDs in Figure S5 (from $n \geq 10$ videos over 3 independent samples).

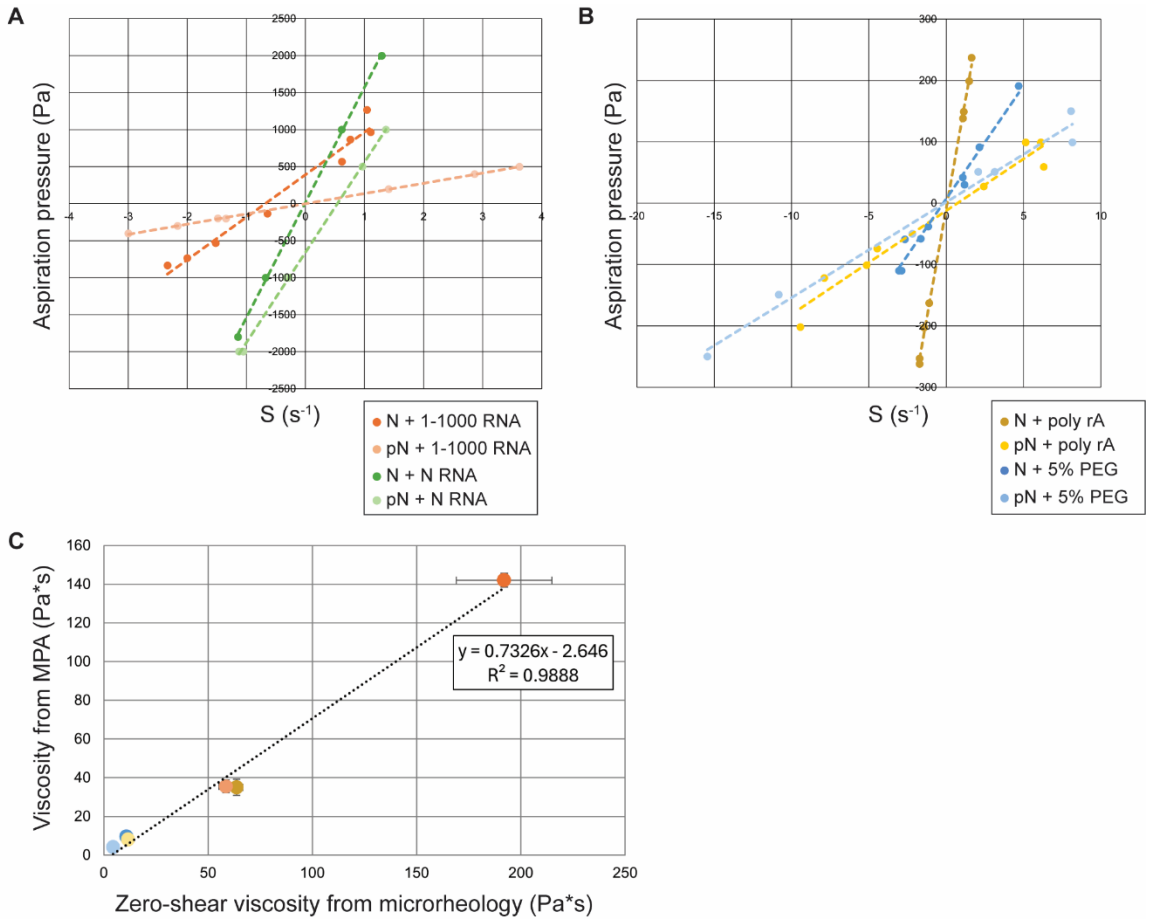

Figure S7. Micropipette aspiration (MPA) of N/pN protein condensates. A) The relationship between aspiration pressure and shear rate S, defined as $S = d(Lp/Rp)^2/dt$, where Lp is the aspiration length, Rp is the radius of the pipette, and t is time, for N or pN condensates with viral RNA. The viscosity is calculated as the slope of the best fit line divided by 4. Data is plotted in Figure 4I. B) Aspiration pressure vs. shear rate S for N or pN condensates with 5% PEG-8000 and 1 mg/mL polyA RNA. C) Comparison of viscosities measured for each N and pN condensate via MPA and microrheology. The trend in viscosities for the condensate compositions tested is consistent between the two methods, but MPA measurements were consistently lower than microrheology measurements. Plotted against each other, we obtain a slope of 0.72 and an R^2 fit of 0.99.

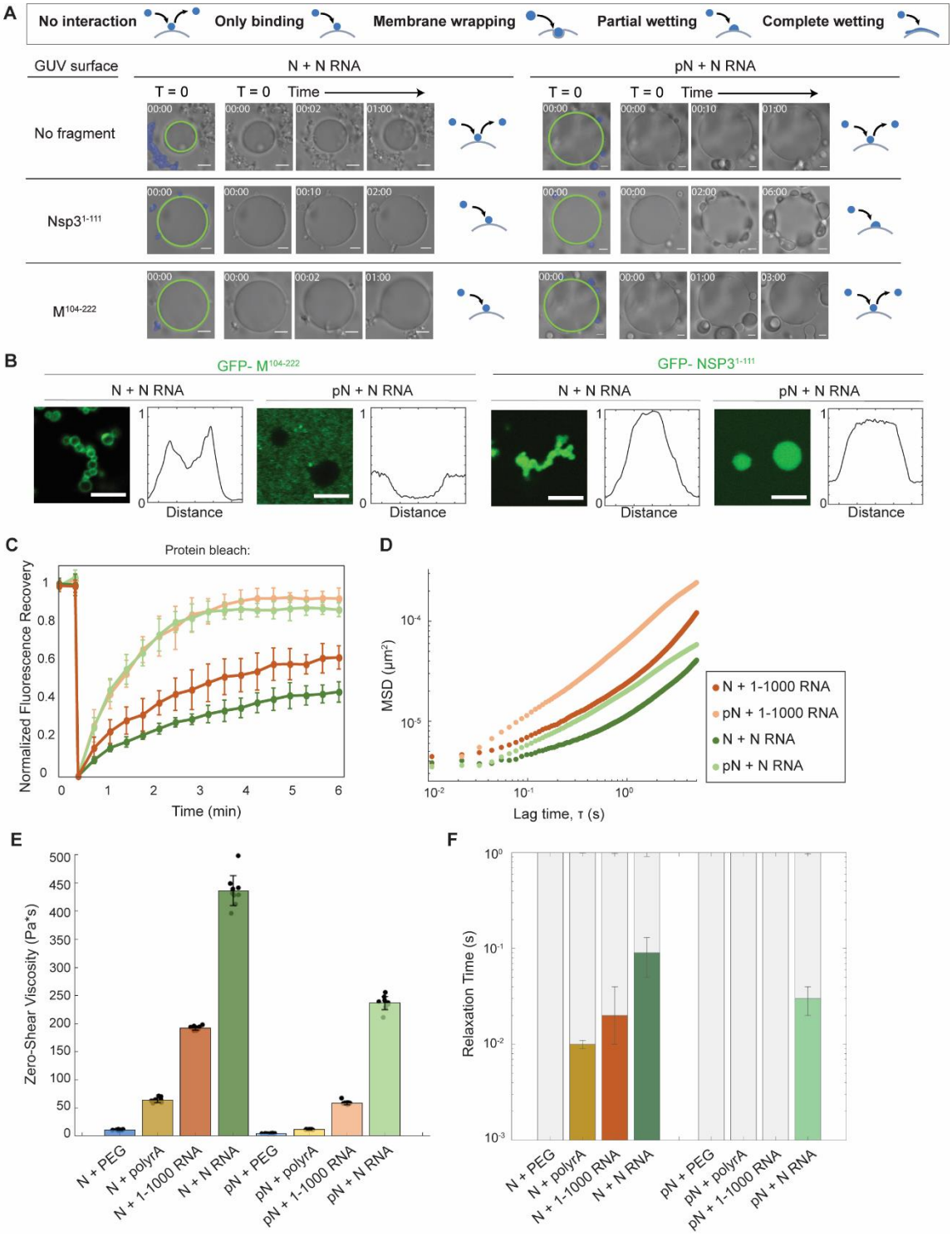

Figure S8. Repetition of material property experiments with N RNA. A) These experiments assess how condensates formed from N or pN protein plus N RNA interact with membranes. Using optical tweezers, condensates are trapped and brought to the surface of GUVs. GUVs have either no protein fragment or GFP-Nsp3$^{1-111}$ or GFP-M$^{104-222}$ displayed at their surface. Representative images show N or pN condensates with N RNA do not interact with naked membranes, but do bind to and may wet the surface of GUVs with Nsp3 depending on the N protein phosphorylation status. Condensates with N but not pN interact with GUVs with the M

protein fragment. B) Interaction between N and membrane protein fragments was confirmed using a partitioning experiment. C) Fluorescence recovery after photobleaching with N/pN and N RNA compared to N/pN and 1-1000 RNA. Unmodified N has lower mobility when condensed with N RNA (recovery half-life = 3.5 ± 0.1 min), compared to with 1-1000 RNA (recovery half-life = 2.6 ± 0.1 min). pN recovery curves are similar across RNA samples (pN + 1-1000 RNA recovery half-life = 1.6 ± 0.1 min vs. 1.4 ± 0.1 for N RNA. D) Ensemble MSD versus lag time for N or pN and N RNA vs. 1-1000 RNA. E) The zero-shear viscosity of the protein and RNA condensates studied, calculated from the particle-tracking results after noise correction. Data from $n \geq 10$ videos from 3 independent trials. F) Quantification of the timescales at which the elastic modulus dominates (color) versus the viscous modulus dominates (grey) in protein and RNA condensates. Error bars represent one standard deviation (±1 s.d.).

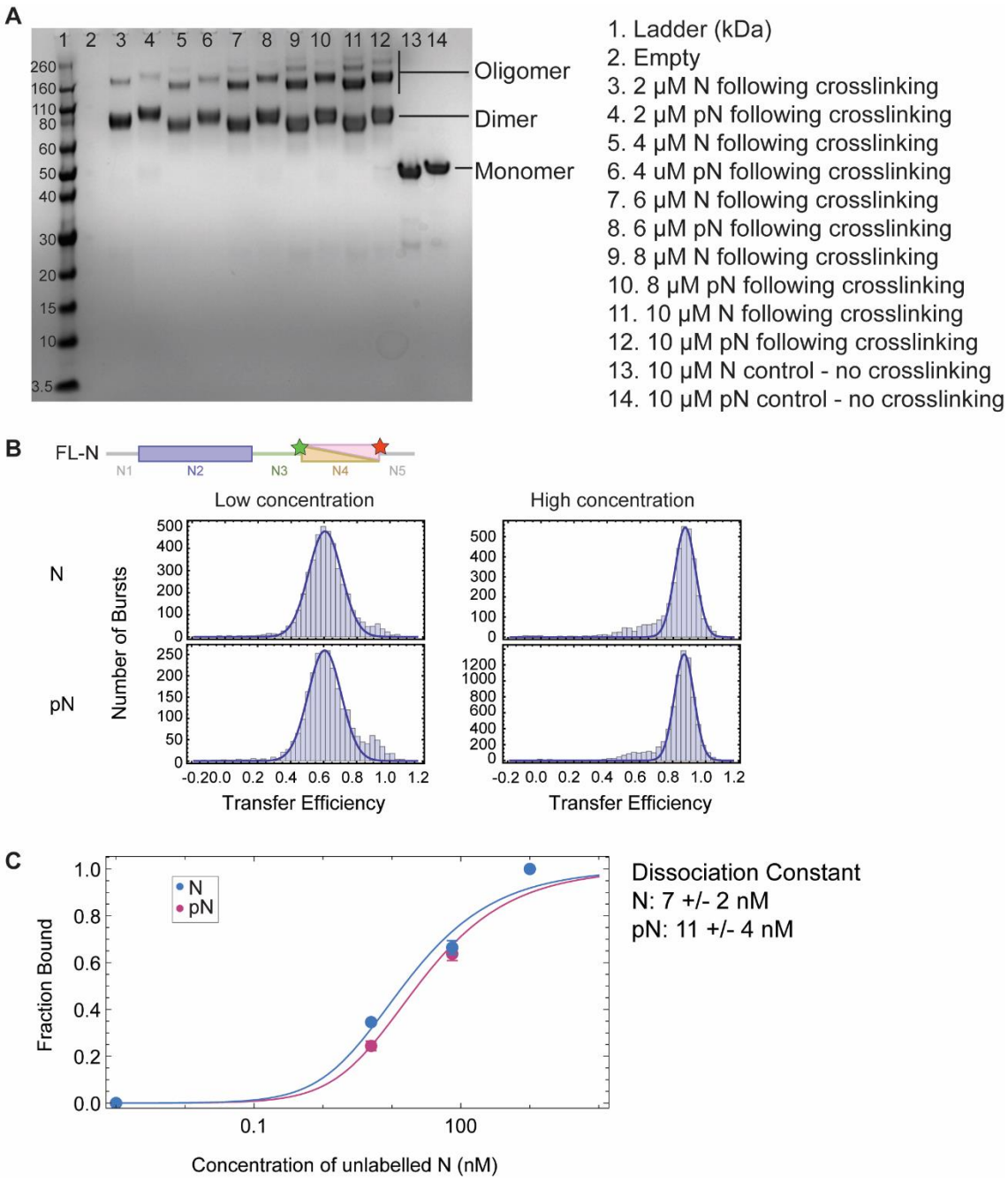

Figure S9. Dimerization and oligomerization analysis for N vs. pN. A) SDS-PAGE gel shows N vs. pN protein (at increasing concentrations) following chemical crosslinking. Crosslinking retains dimer / oligomer state in denaturing conditions of SDS-PAGE. N or pN protein is crosslinked using Bissulfosuccinimidyl suberate (BS3). SDS-PAGE separates oligomers by size. Increasing concentrations of protein results in a greater degree of oligomerization, but phosphorylation has little effect on oligomerization. B) Analysis of the dimerization domain conformation using smFRET. A full-length construct of N was labeled at positions 245 and 363 flanking the dimerization domain. Transfer efficiencies are similar for unmodified and phosphorylated N protein at low concentration (100 pm labeled protein, monomer regime) and high concentration (100 pm labeled + 1 μM unlabeled protein, dimer regime), indicating no shift in conformation of the dimerization domain occurs upon phosphorylation. C) Using a full-length construct that is single labeled at position 363, we measured the dimerization constant for N vs.

pN protein. Binding isotherms of dimerization for N vs. pN indicate a small shift in dissociation constant (quantified to the right). Binding experiments have been analyzed accounting for the possibility of forming dimers of labeled molecules with other labeled molecules, labeled molecules with other unlabeled molecules, as well as between unlabeled molecules, according to the equation developed in Cubuk et al, 2024[1]. Error bars represent one standard deviation (±1 s.d.).

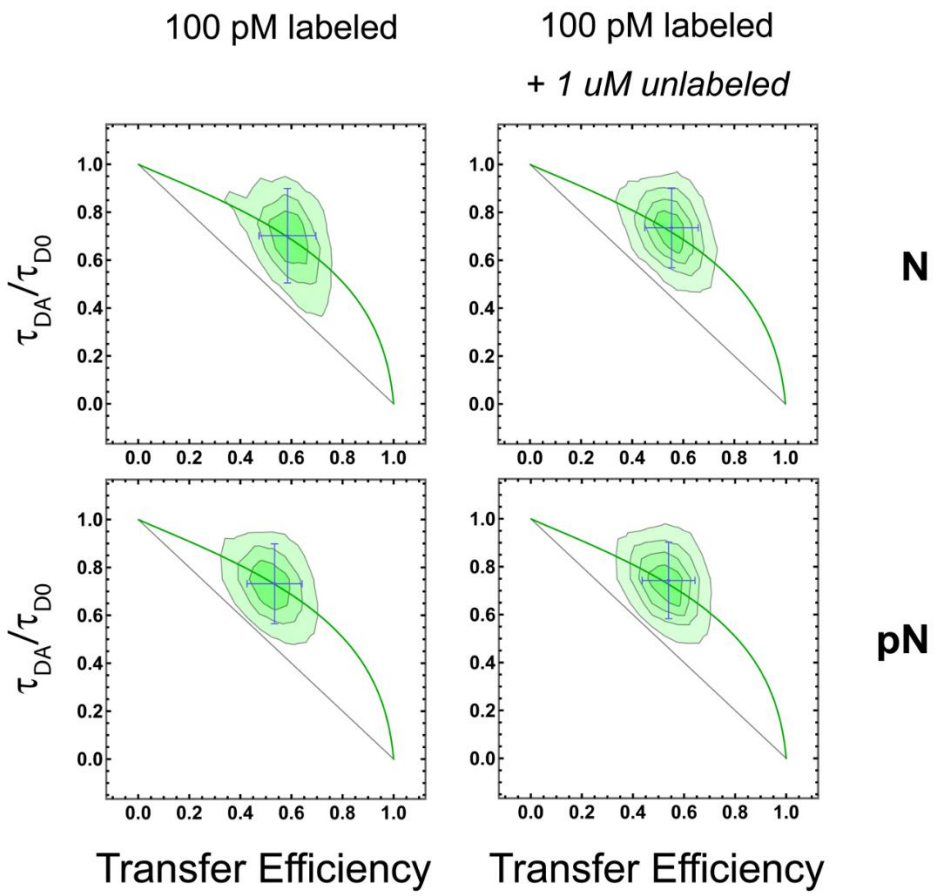

Figure S10. Measuring the dynamic nature of the linker domain by assessing the dependence of fluorescence lifetime on transfer efficiency. Comparison of fluorescence lifetimes for the full-length N in its unmodified and phosphorylated states with fluorophores flanking the central linker at positions 172 and 245. Two concentrations were tested, (1) 100 pM labeled protein as the monomer regime, (2) 100 pM labeled protein + 1 µM unlabeled protein where dimerization is expected. Grey line: linear dependence is expected for a rigid molecule. Green line: the donor lifetime (normalized by the donor lifetime in absence of acceptor: τ_{DA}/τ_{D0}) in the limit of dynamics much faster than the burst duration but slower than the fluorophore lifetime. In all cases, the populations sit near the dynamic line (green) as opposed to falling on the static line (gray), indicating the linker domain remains dynamic in both concentrations and regardless of phosphorylation status.

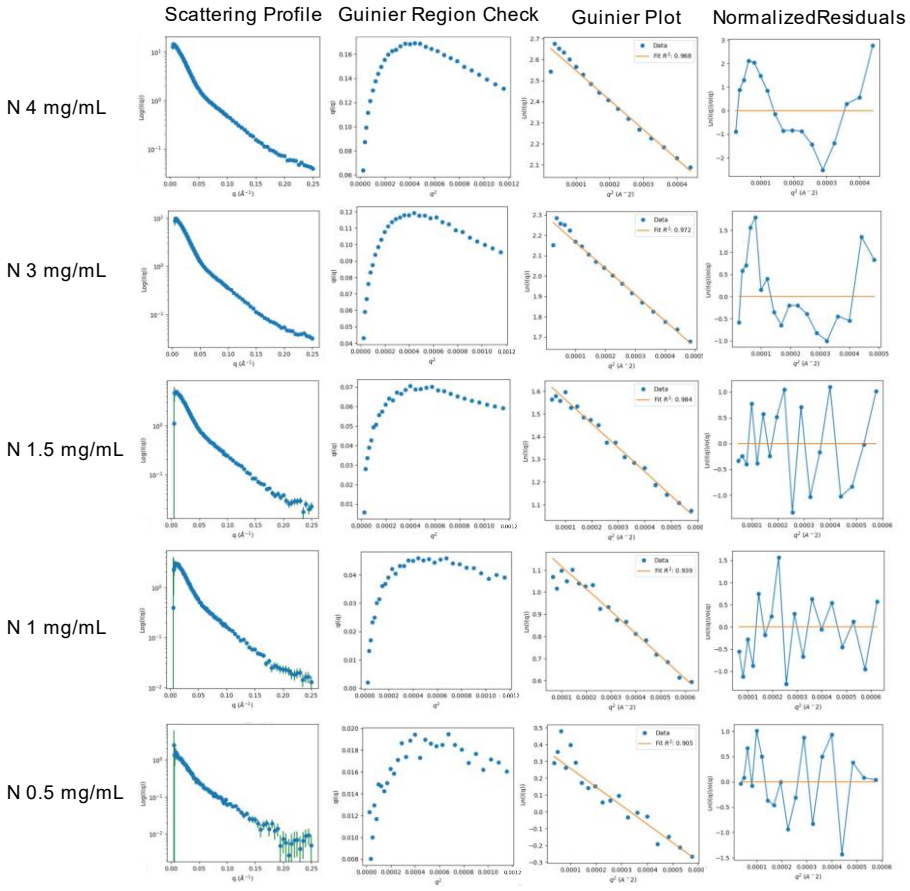

Figure S11. Extended data for Small Angle X-Ray Scattering experiments for unmodified N protein at different concentrations. First column, raw data in the form of scattering profiles. Second column, the Guinier peak analysis plot indicates the validity of doing the Guinier analysis in the third column[2]. Fourth column, analysis that the normalized residuals are randomly distributed about zero.

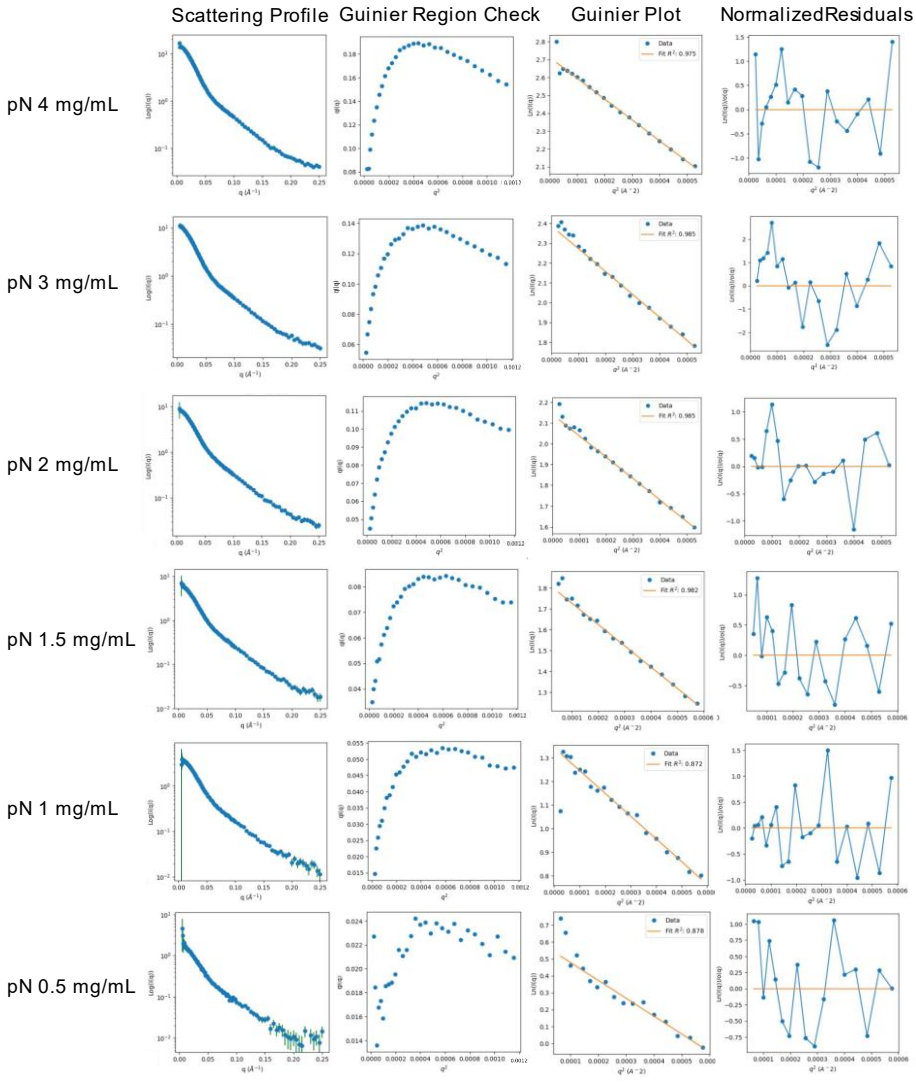

Figure S12. Extended data for Small Angle X-Ray Scattering experiments for phosphorylated N protein at different concentrations. First column, raw data in the form of scattering profiles. Second column, the Guinier peak analysis plot indicates the validity of doing the Guinier analysis in the third column[2]. Fourth column, analysis that the normalized residuals are randomly distributed about zero.

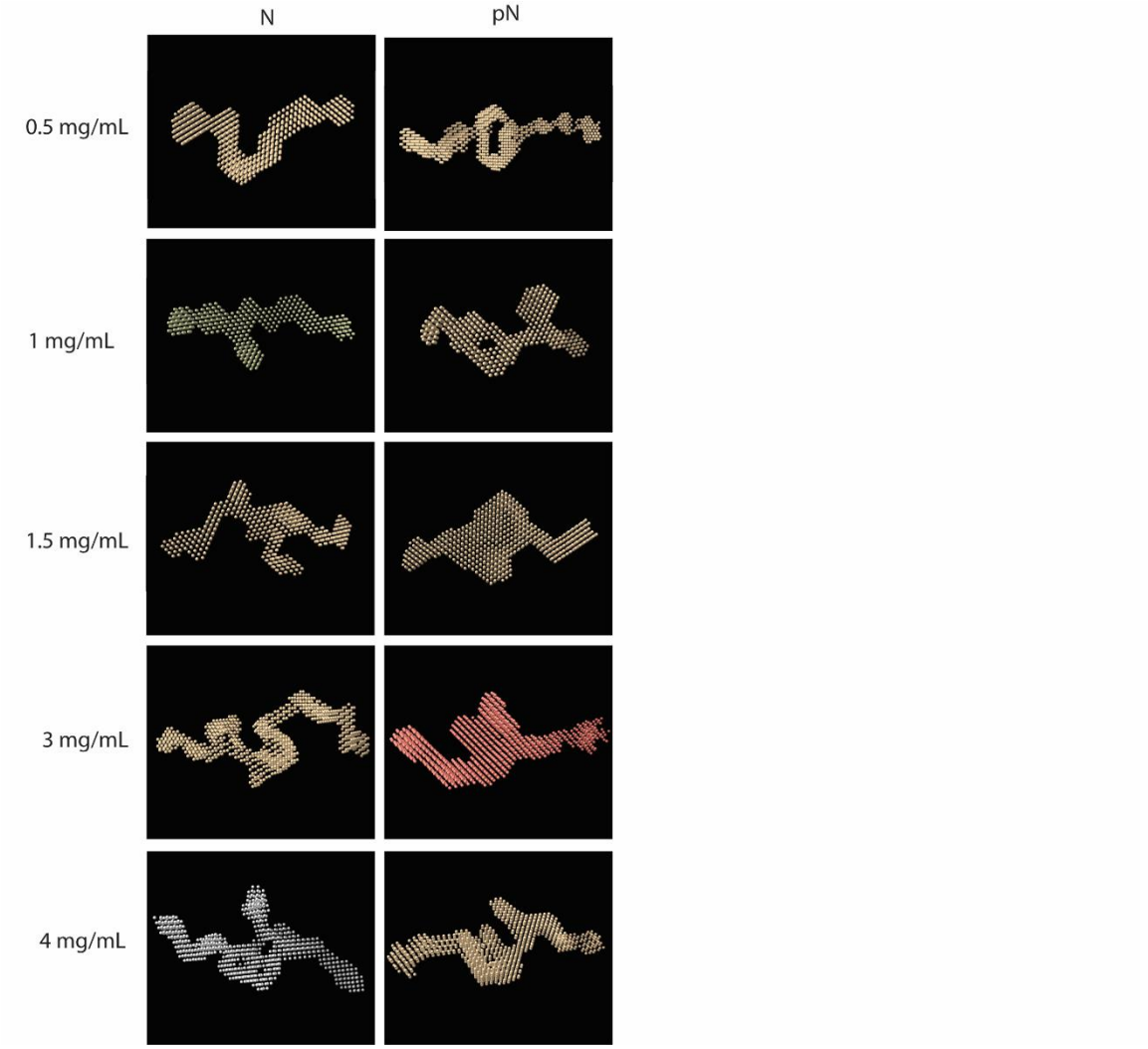

Figure S13. Bead model representations for N and pN from SAXS data at varying protein concentrations.

Supporting Methods

LC-MS: A sample with protein at a concentration of 10 µM was dissolved in 50% ammonium acetate solution and diluted 1:10 fold. The sample was then transferred into an LC vial. Reverse phase liquid chromatography (RPLC) was performed on an Acquity column BEH -C4 -300A˚, 1.7 micron (300 µm x 100 mm, Waters Corporation). Column temperature was set at 40˚C. The following mobile phases were used A: Water with 0.1% formic acid; B: acetonitrile with 0.1% formic acid. The M-Class micro flow LC (Waters Instruments) was operated at a flow rate of 8 µL/min, and 5 µL of sample was injected with an autosampler after equilibration of the column. For the separation of proteins, the following concentration gradients were used: starting with 5 – 90% B for 55 minutes and then back to 5% B for minutes 55 - 62. Prior to injection on the RPLC column, a blank run was performed. ESI-MS experiments were performed using a quadrupole-TWIMS-TOF hybrid mass spectrometer (Synapt G2 HDMS; Waters Corporation) in positive ionization mode with m/z scan range 400 - 4000. The applied experimental parameters were capillary voltage, 3.0 kV; sampling cone voltage, 40 V; source offset 80˚C; source temperature, 100°C; desolvation temperature 250˚C; cone gas 50 L/Hr and desolvation gas 600 L/Hr. Data analysis was performed using MassLynx 4.1 and protein deconvolution was performed using Mas Ent 1.

BS3 Cross-linking Experiment: Protein (2-10 µM in PBS at pH 7.5) was chemically cross-linked with bis(sulfosuccinimidyl) suberate (BS3) (Thermo Fisher) (50 µM) at room temperature for 30 min and quenched by adding Tris (pH 7.5) to a 20 mM final concentration. Reaction mixtures were then analyzed by SDS-PAGE.

smFRET lifetime analysis: Analysis of fluorescence lifetime from mean FRET transfer efficiencies was conducted as described in Cubuk et al. 2024[1].

smFRET dimerization constant: Modeling of dimerization was conducted as described in Cubuk et al. 2024[1].

Bibliography

1. Cubuk, J. *et al.* The dimerization domain of SARS CoV 2 Nucleocapsid protein is partially disordered as a monomer and forms a high affinity dynamic complex. *bioRxiv* (2024).

2. Putnam, C. D. Guinier peak analysis for visual and automated inspection of small-Angle X-ray scattering data. *J. Appl. Crystallogr.* **49**, 1412–1419 (2016).